1-1-2002

Super hard boride thin films on carbide inserts for metal cutting

Ramachand Cherukuri
Iowa State University

Super hard boride thin films on carbide inserts for metal cutting

by

Ramachand Cherukuri

A thesis submitted to the graduate faculty

in partial fulfillment of the requirements for the degree of

MASTER OF SCIENCE

Major: Mechanical Engineering

Program of Study Committee:

Palaniappa A Molian (Major Professor)
Daniel Bullen
Shashi Gadia

Iowa State University

Ames, Iowa

2002

Graduate College
Iowa State University

This is certify that the master's thesis of

Ramachand Cherukuri

has met the thesis requirements for Iowa State University

Signatures have been redacted for privacy

to

the cherukuri family
&
mastan annayya

TABLE OF CONTENTS

Acknowledgements

I would like to thank the support and encouragement provided by Dr.Molian during the course of my study at Iowa State University. His support in helping me pursue a minor in Computer Science along with masters in Mechanical Engineering helped me greatly in my career. I would also like to thank Dr. Bullen for kindly accepting to be on my committee and Dr. Gadia for being graduate minor representative in Computer Science. I would also like to thank Larry Couture for his technical assistance in operating CNC lathe and my friends Diwakar, Melissa and Wenping for their support.

CHAPTER 1. GENERAL INTRODUCTION

Machining (material removal) is one of the important processes of the manufacturing industry. Because of the presence of high temperatures, frictional forces, tools degrade gradually and this phenomenon is called wear. The frequent replacements of tools required during the cutting operation results in the loss of precious time, requires more labor and hence more cost of the manufacturing.

Flank, crater, and nose wear influence the cutting operation and hence have adverse effects on the workpiece being machined. Flank wear is usually attributed to the high temperatures involved in the cutting process and also due to the sliding of the tool on the workpiece where as crater wear is caused by high temperatures and also the chemical affinity between the tool and the workpiece. The higher the tool-chip interface temperature, higher is the tool wear.

In order to reduce the wear rate and improve the efficiency of cutting tools, different types of cutting tool materials are deployed in the machining process depending on the material being machined. The following properties are considered while choosing various cutting tool materials: hardness at high temperatures, toughness, wear resistance, chemical inertness and good bonding to the substrate. Hardness at high temperatures helps to maintain the strength, toughness to withstand the vibrations and shocks involved in the intermittent cutting process, chemical inertness to avoid reactions with the workpiece and thereby contributing to the reduction in wear and good bonding to the substrate to prevent flaking.

Wide ranges of tool materials have been developed for use in machining. Some of the most widely used tools are carbides, ceramics and high-speed steels. Also diamond and cubic boron nitride are used as coating materials to take advantage of their high hardness characteristic.

Carbide tools are considered to be the most cost effective of all the available tools because of their high hardness over a wide range of temperatures and other properties like high thermal conductivity and low thermal expansion. There are two different types of carbide tools available in general, tungsten carbides and titanium carbides. Tungsten carbides, which are also called as cemented carbides, are developed using powder metallurgy techniques, mixing WC with Cobalt. As the amount of cobalt is increased, strength, hardness and wear resistance decreased but toughness increases. Tungsten carbides are typically used for cutting steels, cast irons and abrasive non-ferrous metals. Titanium carbide tools possess high wear resistance but less toughness than WC tools. They are typically used in the machining hard materials like steel and cast irons, and for cutting at speeds higher than those for tungsten carbides.

The introduction of cutting tool inserts is considered to be a revolutionary change in the history of cutting tools, which led to an increase in productivity. Different types of cutting tool inserts have been developed. Introduction of coated carbides has led to high efficiency in the cutting tools.

Coating acts to reduce the tool wear, cutting forces, cutting edge temperatures, and increase abrasion resistance. It also acts as diffusion barrier by preventing the contact between the chip and the cutting tool and also as lubricants by reducing the friction between the tool and the workpiece. Coatings are classified as single layer coatings, and multilayer coatings. Multilayer coatings are used to improve hardness and toughness. The use of different functional intermediate layers in multilayer coatings helps to obtain various properties of the different cutting materials like hardness, high thermal stability and low friction. In some cases, coating materials, which provide good bonding to the substrate are used as an interfacial layer between substrate and the actual coating.

Vapor deposition, one of the most important coating methods, includes the following steps.

- Creation of vapor phase species by thermal or kinetic energy
- Transport of vapor species from source to substrate
- Film growth on the substrate.

The different types of vapor deposition mechanisms are Physical Vapor Deposition (PVD), Chemical Vapor Deposition (CVD), and Pulsed Laser Deposition (PLD). Each method has its own advantages and disadvantages and the choice of a particular deposition technique depending on the materials being coated and the application of the coated tool. In PVD, small coating thickness (3 to 5 μm) works well on sharp-edge tools than thicker coating. Also, low temperatures involved in the process do not adversely affect the underlying properties of the substrate.

In PLD, a plasma is formed by laser interaction with the target and it contains ionized atoms or molecules of the target material. The interaction of plasma with the laser beam, causes heat transfer to plasma plume and it expands rapidly. This plasma gets deposited on the substrate. The deposition rate, thickness and quality of film are determined by the laser parameters like focal spot of the laser beam incident on the target, pulse repetition rate of the laser beam, pulse width, laser wavelength, distance of the substrate from the target and substrate temperature. Nd:YAG and Excimer lasers are used typically used lasers for PLD process.

Thesis Organization

The thesis is organized into four chapters. Chapter 2, a paper accepted for publication by the Journal of Surface and Coatings Technology presents the feasibility of coating $AlMgB_{14}$ on cutting inserts and also presents the machining of 1045 steels using coated and uncoated carbide (C-5 and C-2) tools. Chapter 3, a paper submitted for review and publication in the Journal of Machining Science and Technology, describes the details of machining Ti-6Al-4V alloy using coated and uncoated carbide inserts along with the results for flank wear, nose wear and surface roughness. Chapter 4 presents the major conclusions.

CHAPTER 2. PULSED LASER DEPOSITION OF $AlMgB_{14}$ ON CARBIDE INSERTS FOR METAL CUTTING

A paper accepted by the Journal of Surface and Coatings Technology

*[1]Ram Cherukuri, *Melissa Womack Shibata, *Pal Molian, **Alan Russell, **Yun Tian

ABSTRACT

Nanocrystalline $AlMgB_{14}$ containing 0 to 30 mol% additives are a family of *new superhard materials* with hardness comparable to that of TiB_2 on the lower end and to that of cubic BN on the higher end. Compared with diamond and cubic BN, $AlMgB_{14}$ is an equilibrium material with excellent electrical conductivity, high chemical stability, and lower density. The projected cost of manufacture of the boride is 10% of the cost of diamond and cubic BN. $AlMgB_{14}$ materials appear to be congruently melting/evaporating, which would allow them to be processed with techniques such as *Pulsed Laser Deposition (PLD).*

In this work, the feasibility of PLD for synthesizing thin films of baseline $AlMgB_{14}$ (0% additive) is demonstrated and compared with TiB_2. A 248-nm, 23-ns KrF excimer laser was used to prepare baseline boride thin films on cemented carbide (ANSI C-5 and C-2) tool inserts. The films were dark blue, continuous and fairly uniform with few particulates. An

---

* Department of Mechanical Engineering, Iowa State University, Ames, IA 50011, USA

** Department of Material Science Engineering, Iowa State University, Ames, IA 50014, USA

[1] For communication, contact ramcc@iastate.edu

impact fracture test showed hardness 60% higher than the carbide substrate. Lathe turning tests with cold-drawn 1045 steel bars indicated that C-5 tools coated with 0.5 μm baseline $AlMgB_{14}$ have an average flank wear reduction of 12% compared to uncoated C-5 tools. Further machining tests on C-2 tools showed that the tools coated with baseline boride have much better flank (23 % reduction) and nose wear resistance (26 % reduction) compared with TiB_2 coated tools. In addition, multilayer composite coating of $AlMgB_{14}$ and TiB_2 outperformed single layer boride coating in minimizing the tool wear. This pioneering work sets the stage and serves as a catalyst for rapid and innovative advances in the development of new boride materials for numerous tool and hard coating applications, including bulk cutting tools, hard and erosion-resistant coatings, wear-resistant electrical switch contacts, and conductive thin films for MEMS.

Keywords: [C] Pulsed laser deposition (PLD), [D] Multilayer, [X] Boride, [A] Scanning electron microscopy (SEM).

INTRODUCTION

Continued advances with respect to quality, flexibility, productivity, and environmental concerns brought new machining technologies, including high speed machining, hard turning, precision machining, dry machining and environmentally conscious machining. Successful implementation of many of these processes demand high performance from the cutting tools. An issue of great concern regarding cutting tools is their wear resistance. Mechanisms such as adhesion, abrasion, oxidation, diffusion and fatigue,

caused by complex stresses, as well as heat generation due to shear deformation and friction, recount for the failure of tools used in machining tasks.

A cutting tool must possess a high degree of hardness, toughness, and chemical compatibility, and a low degree of friction. Abrasive wear on the flank and clearance faces can be reduced by increased tool hardness, while raising the tool toughness can prevent catastrophic breakage. Crater wear can be minimized by suppressing chemical interactions between the cut chip and the tool surface, while the built-up edge (BUE) can be reduced by decreasing friction. Recent advances in cutting tool technology have shown that the application of thin coatings at the tool edges can substantially enhance the tool properties. Basically, three types of hard coatings used in tools, in decreasing order of popularity [1-4], are: 1) Ti-based coating materials such as TiN, TiC, (Ti,Al)N and Ti (C,N); 2) Ceramic coatings, mostly of the type Al_2O_3; 3) Superhard coatings like CVD-diamond and cubic boron nitride (cBN). The Ti-based coatings exhibit good bonding to the substrate and offer moderate mechanical and thermal properties with an adequate rate of deposition. Ceramic coatings provide thermal stability and higher resistance to abrasive wear but suffer from brittleness and poor bonding to the tool substrate. Diamond coatings, although they have several benefits with regard to surface finish, built-up edge, cutting forces, and tool life, do not adhere well to tool substrates.

The modern trend is to use multilayer coatings tailored to combat different types of wear. In a typical TiC/ Al_2O_3 /TiN multilayer coating applied by CVD technique, TiC resists abrasive flank wear, Al_2O_3 provides good chemical protection for the rake face, and TiN

provides lower friction as well higher hardness. These multilayer coatings have phenomenal success with respect to speed and tool life improvements [1-5]. Another development in multilayer coating is use of a large number of alternating thin layers to reduce the propagation of cracks and to yield finer grain sizes leading to higher hardness [5]. New developments in tool coatings include "superlattice" and "multielement" coatings [1]. Superlattice coatings are essentially nanocomposites in which alternate layers of two hard materials, such as TiN/NbN, are embedded in nanoscale thickness. Unlike multilayer coatings, the multielement coating consists of eight different elements combined into one superthin coating [1]. Both these developments offer greater tool life improvements (five to seven times) than traditional Ti-based coatings.

Advancements in coatings and coating technology are needed for continuous quality improvements in the machine tool industry as demand for high-speed machining and difficult-to-machine materials evolves. Recently, a family of new lightweight, intermetallic materials with the composition $AlMgB_{14}$ containing 0 to 30 mol % additives, was reported by scientists at the Ames Laboratory [6]. The extreme hardness of these thermodynamically stable materials could be used for tool and protective coating applications. Microhardness and density data, listed in Table 2.1, indicate that $AlMgB_{14}$ fall in the category of lightweight, ultra-hard materials, comparable to TiB_2 and cubic BN (cBN).

$AlMgB_{14}$ differs from diamond and cBN with regard to crystal structure, state of equilibrium, electrical conductivity, and property changes brought about by additives. Diamond and cBN have simple, symmetric, isotropic crystal structures, whereas the

Table 2.1. Hardness and Density of Superhard Materials [1]

Material	Hardness, Gpa	Density, g/cm^3
Diamond	70	3.52
CBN	45-50	3.48
TiB_2	30-33	4.50
TiC	28-29	4.93
SiC	24-28	3.22
Al_2O_3	21-22	3.98
Si_3N_4	17-21	3.19
* $AlMgB_{14}$	32-35	2.66
*$AlMgB_{14}$ + Si	35-40	2.67
*$AlMgB_{14}$ + TiB_2	40-46	2.70

*Data from Ames Laboratory based on a large number of tests.

orthorhombic structure of baseline $AlMgB_{14}$ is quite complex although its low symmetry, 64 atoms per unit cell, and incompletely occupied atom sites all appear to contradict the accepted precepts for extreme hardness. Nevertheless, the baseline material is among the hardest bulk substances known. Its ability to increase in hardness when other elements and compounds are added suggests that its physical properties can be optimized by suitable changes in composition and processing. The electrical conductivity of $AlMgB_{14}$ (resistivity = 1.2 to 7.2 x 10^{-4} ohm-cm) is much higher than that of other ultra-hard materials and nearly the same as that of polysilicon. Chemical reactivity tests at Ames Laboratory have

demonstrated that these materials show little reactivity to carbon steel, stainless steel, and titanium at temperatures as high as 1300°C [6].

The cost of boride is much lower than that of diamond or cBN. Depending on particle size and grade, diamond and cBN powders cost from $2000/kg to $15,000/kg. The principal cost in producing boride material is that of boron, at about $200/kg to $ 1500/kg with increasing purity. Costs of other elements such as Al and Mg and costs associated with milling and sintering will bring the cost of the boride to about $400/kg to $2000/kg.

$AlMgB_{14}$ materials could be successfully used as coating materials because of their stability at high-temperature, unique combinations of properties, favorable cost, and availability. These coatings could be applied as thick films by thermal spray techniques or as thin films by *Pulsed Laser Deposition* (PLD) methods. It is suspected that thermal spray techniques tend to disintegrate the stochiometry of the starting powder because of differences in vapor pressures of the elements as well as the complex solidification path. In contrast, PLD techniques can preserve the stochiometry of films because of congruent melting/evaporating characteristic resulting from deposition of depositing of species such as atoms, ions, and clusters on a pre-heated substrate. In this work, a pulsed laser deposition (PLD) technique was used to deposit 0.5 to 1-μm thin films of $AlMgB_{14}$, TiB_2, and $AlMgB_{14}/TiB_2$ on ANSI C-5 and C-2 carbide inserts. The films were characterized and evaluated for metal cutting application.

PULSED LASER DEPOSITION

Pulsed laser deposition (PLD) is a conceptually and experimentally simple yet highly versatile technique for thin film applications. In PLD (Figure 2.1), a target inside a vacuum chamber is irradiated by an intense source of laser radiation, creating a plasma plume. The plume then flies off the target surface and condenses onto the material to be coated (substrate). PLD has several beneficial characteristics, listed below, which distinguish it from other thin film growth methods [7-11]: 1) Congruent ablation - rapid heating of the target and rapid cooling of the film on the substrate do not allow dissociation of source material, even though the constituents have different vapor pressures, leading to stoichiometric films; 2) High kinetic energy species - the ionized and excited species ablated by the laser have high kinetic energy and velocities (10^6-10^7 cm/sec) and thereby promote film crystallinity and dense packing; 3) Uniformity – the plume developed during the ablation is in a cone and assists in attaining films of uniform thickness in a narrow zone; and 4) High purity films - low heat input followed by local evaporation tends to produce high purity films; high energy fluence "burn" the impurities.

PLD has experienced explosive growth in the past decade, especially since its successful use with superconducting oxides. It has been employed in the preparation of high quality dielectric films, epitaxial semiconductor layers, superlattices and ceramics, nanocrystalline materials, ferroelectrics, amorphous diamond, tribological coatings and polymers [7-11]. PLD is a scientifically challenging process because aspects such as laser-target interactions (evaporation of the target and plasma formation by laser energy absorption

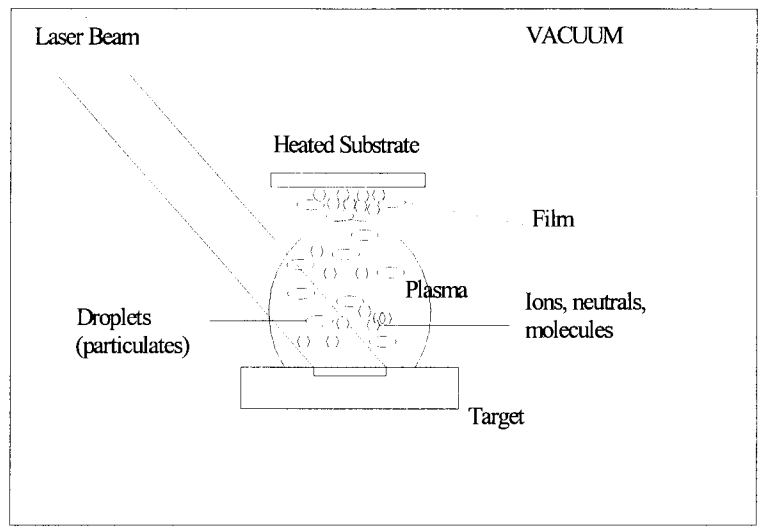

Figure 2.1. A schematic pulsed laser deposition process.

followed by isothermal expansion), as well as the non-equilibrium processes governing species interactions and the subsequent nucleation and growth of thin films are not fully understood. Despite the existence of a large body of literature, there is still no coherent picture of the fundamental mechanisms.

Excimer lasers are mostly used for PLD because of their short wavelengths (193-351 nm), high energy per pulse (0.1 to 2 J) and nanosecond (10-30 ns) pulse widths, although Q-switched Nd:YAG lasers in the frequency-tripled or quadrupled modes with pulse duration of 4-12 ns may also be used.

EXPERIMENTAL PROCEDURE

Materials

The substrates selected for deposition were ANSI C-5 and C-2 carbide tool inserts. C-5 is a steel cutting grade that consists of WC-Co, with some TiC and TaC. The C-5 triangular insert with an included angle of 60° was obtained from Kennametal, Inc. The tool geometry is *–5,-5,5,5,15,15, 1/32.* The C-2 insert has a rhomboidal shape with an included angle of 80° and with a chip-breaker groove. It is a straight WC-6%Co with a grain size of 1 μm (Grade 883) supplied by Carboloy-Seco, Inc. The tool designation is CNMG 432-MR4 having a negative land geometry with high edge strength. The tool geometry consists of rake angle –6°, relief angle 6°, lead angle 13°, and nose radius of 0.8 mm (1/32 in.). The cemented carbides were chosen because more than 70% of all cemented carbide inserts feature coatings applied by chemical vapor deposition (CVD) or physical vapor deposition (PVD) or a combination of the two [5]. The surfaces of substrates were degreased in trichloroethylene and ultrasonically cleaned in methanol.

The target material was the *baseline* $AlMgB_{14}$ which, with an average hardness of 2100 HV, is harder than the carbide substrates (< 1700 HV). The target material was prepared by mixing 2.24 gm of B, 0.36 gm of Mg, and 0.4 gm of Al and ball milling the mixture for 12 hours. The powdered mixture was subjected to uniaxial hot pressing and sintering at 1400°C for 60 minutes. The target was then polished and made available in the form of 12-mm diameter, 3-mm thick discs. The target was characterized as to composition ($AlMgB_{14}$), hardness (1800-2400 HV), density (2.466 gm/cm^3), and nanocrystalline

structure. In addition to $AlMgB_{14}$, commercially available 99.5% purity TiB_2 target (SS 261, Cerac Inc., Wisconsin) was obtained for the purpose of comparison of tool wear.

Experimental Set-up and Processing

Pulsed laser deposition experiments were performed in a high-vacuum ($133.3*10^{-6}$ Pa) stainless steel chamber equipped with four vacuum ports and a quartz window that allowed observation of plasma. Diffusion pumps ensured vacuum. The deposition chamber has provisions for the laser beam window, gas flow, heating of the substrate up to 500°C, and mounting of the target. The laser beam was made to focus on the target at a 45° angle of incidence, with a resulting elliptical spot. During ablation, the target was rotated using a magnetic controlled device. The rotation is needed to prevent cratering of the target by the laser beam and to minimize particulate formation. The tool edge (substrate) was oriented normal to the substrate, and the substrate-to-target distance was 43 mm. The substrate was preheated to 500°C and the deposition process was facilitated by a computerized control system in which the laser parameters (power, pulses and shutter), target rotation, target-to-substrate distance, and substrate temperature were controlled. The following parameters were used for obtaining thin films in the thickness range of 0.2 to 1.5 μm. Table 2.2 summarizes the coatings applied on the tools.

Table 2.2. Sample Designations of Coated Tools

Sample Designation	**ANSI Tool**	**Deposition time**	**Coating**
A	C-5	30 minutes (single layer)	$AlMgB_{14}$
B	C-2	45 minutes (single layer)	TiB_2
M	C-2	45 minutes (single layer)	$AlMgB_{14}$
L	C-2	45 minutes each (double layer)	$AlMgB_{14} + TiB_2$

Laser: KrF excimer

Wavelength: 248 nm

Pulse Width: 23 ns

Repetition Rate: 5 Hz

Pulse Energy: 200 mJ

Spot area: 2.8 mm^2

Deposition time: 10 minutes to 60 minutes

Characterization

An Amray scanning electron microscope (SEM) was used to examine the microstructure and surface morphology of the samples at an operating voltage of 10 kV with secondary electrons. Energy dispersive spectroscopy (EDS) was employed to determine the

composition on the sample surface. A DEKTAK surface profilometer was used to measure the film thickness.

Nanoindentation testing with a Berkovich diamond indenter (a three-sided pyramid with an area-to-depth function the same as that of a Vicker's indenter) was used to measure the hardness and elastic modulus of thin films. In this test, the load was gradually increased to a pre-set maximum value such that both elastic and plastic deformation occurred in the thin film. The load was then released, causing partial or complete relaxation. The unloading was dominated by elastic displacements.

Machining Tests

A 20-HP engine lathe was used for conducting turning tests using coated and uncoated C-5 tools. The workpiece was 50 mm diameter cold-drawn AISI 1045 steel with a hardness of 200 HB. The cutting parameters were as follows: feed = 0.2 mm/rev (0.008 in./rev), speed = 164 m/min (537 fpm), depth of cut = 0.76 mm (0.03 in.), dry machining. During machining tests, the flank wear was measured periodically using a toolmaker's microscope. The tests were run for 30 minutes or until the tool was fractured. Tool wear tests were repeated four times on both uncoated and laser deposited C-5 tools. A linear regression analysis was used to determine the significance of reduction in tool wear by the boride coating. A straight line that represents the experimental data was fitted based on standard regression equations. A 95% confidence interval was determined.

A Hitachi Seiki HT 20SII CNC turning center was used to machine steel bars using C-2 grade tools. The lathe has the provision to keep the surface speed constant while the diameters are being reduced. Bars were discarded when the diameter was reduced to 25 mm. No coolant was used during the experiments. The speed and feed were kept constant throughout the experiments. The machining parameters included feed of 0.2 mm (0.08 in.), cutting speed of 92 m/min (300 fpm), and depth of cut of 1 mm (0.04 in.). After each pass the tool was removed from the tool post. Because of the decrease in diameter, the average time taken for each pass varied. The flank and nose wears were measured using Gaertner Scientific toolmaker's microscope with a magnification of 30X. Tests were repeated three times. The ISO's criteria [27] were used for tool life that includes average flank wear 0.4 mm, nose wear 1.0 mm, crater wear depth 0.14 mm, and surface roughness 6 μm Ra. SEM was used to characterize the tool wear.

RESULTS AND DISCUSSION

Profilometry traces of the boride coating showed an average thickness of 1.5 μm for 1-hour deposition. The deposition rate was approximately 0.8 Å per pulse (typical of most PLD). The film was non-uniform, however, smooth and continuous. The plume being highly forward directed causes the nonuniformity in film thickness and its spatial flux being highly nonuniform so that regions near the plume center received more deposition, while regions far from the plume center received less. The thickness distribution of deposited films analyzed by Sajjadi et al. [12], follows the intensity distribution given by:

$$I = IoCos^{n}\theta$$

where θ is the angle relative to the direction normal to the target surface. The central part (a disc of about 1 cm) of the deposited film is generally thicker than the external part because the central part represents contributions of both ionized species and neutral particles, while the external part is the result of the deposition of mostly neutral particles. It is possible to obtain uniform thickness by scanning the laser beam across the target while asynchronously rotating the target.

Figures 2.2 and 2.3 scanning electron micrographs showing the morphology of uncoated and boride-coated C-5 substrate surfaces respectively. The grinding marks on the uncoated surface are readily apparent. The surface of the boride-coated tool appears smoother, with a continuous coverage of thin film and some spherical particles (Figure 2.3b). The occurrence of particulates in thin films is common in PLD and is attributed to the splashing effect. In PLD, liquid droplets from the target are explosively ejected causing formation of micron-sized particulates (the major drawback of PLD) in the film. The ejection of liquid droplets is attributed to superheating of the subsurface layers, solid-liquid phase change, thermal expansion of the material in the region of thermal penetration depth, the recoil pressure on the molten surface generated by the vaporized species, and degradation of the surface. Droplet densities of 10^3 to 10^6 particles/cm^2 have been reported for films about one μm thick [7].

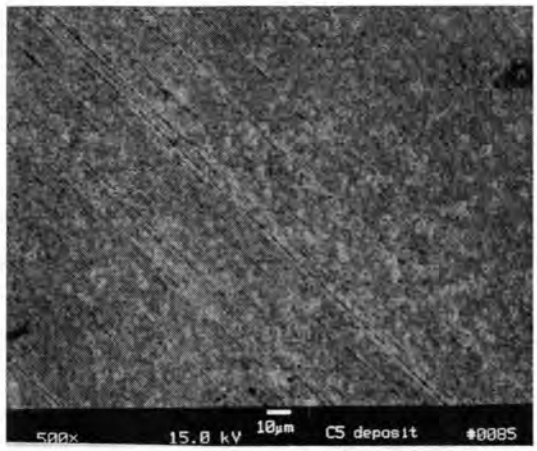

Figure 2.2. Scanning electron micrograph of AISI C-5 Substrate.

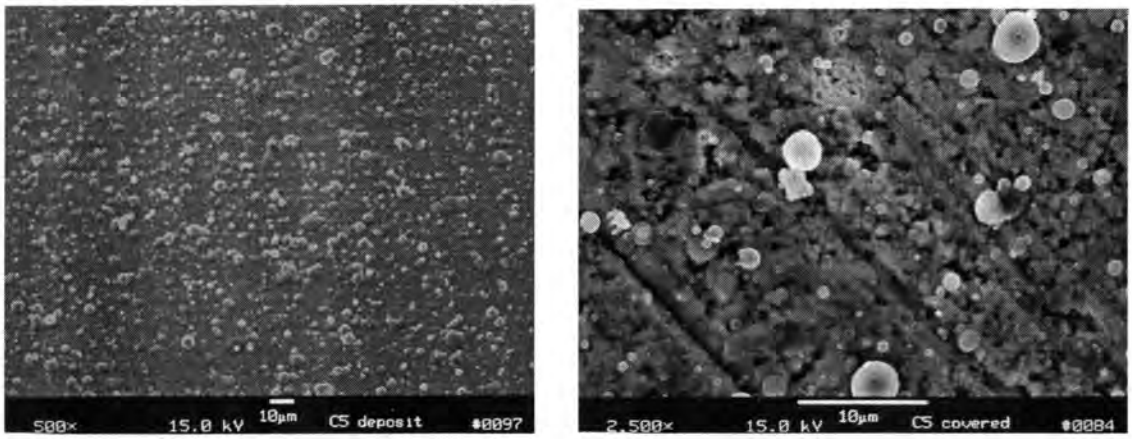

Figure 2.3. Pulsed laser deposited boride film (a) 500 X (b) 2500 X

Figures 2.4a and 2.4b show the energy dispersive spectra (EDS) of substrate and coating respectively. It can be seen that the $AlMgB_{14}$ target material is faithfully reproduced in the film. The EDS spectrum also showed that the films contain oxygen and iron impurities that came from the target and the environment. Although the Al, Mg, and B elements were

shown by EDS to be present in approximately the correct proportions of 1-1-14, this does not necessarily mean that the coating had the desired ultra-hard crystal structure (the oI64 orthorhombic unit cell with four B12 icosahedra). Thin film x-ray diffraction measurements, which will be needed to confirm the existence of the ultra-hard crystal structure in the coatings, are planned for the near future.

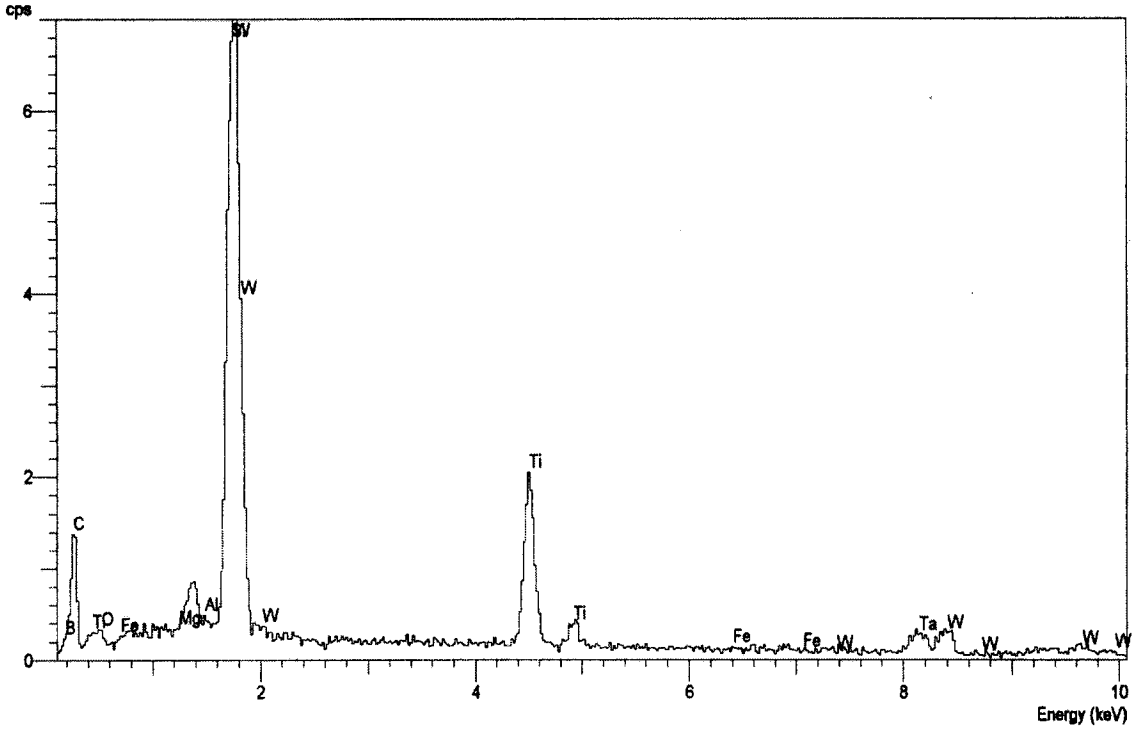

Figure 2.4. (a) EDS spectrum of substrate

Figure 2.5 shows the impact-fractured surface of C-5 coated with $AlMgB_{14}$ for a deposition time of 10 minutes. The smooth fracture surface is an indicator of brittle fracture. The left region consists of sub-micron sized WC particles, while the right region is a uniform thin layer of $AlMgB_{14}$. It can be seen that $AlMgB_{14}$ bonds very well to the substrate. The coating is uniform, dense and adherent even after brittle fracture. The strong adherence is attributed to the high speed of the species that generate a pressure pulse as high as 1 MPa at the surface [11]. Energetic species and supersonic velocity account for adherence and smoothness of films because high-energy species can break atomic bonds, cause thermal spikes, generate subsurface vacancies, enhance adsorbed atom mobility, and generate nucleation centers. Surface diffusion of adsorbed atoms is also enhanced by the impact of highly energetic species, resulting in smoother film morphology.

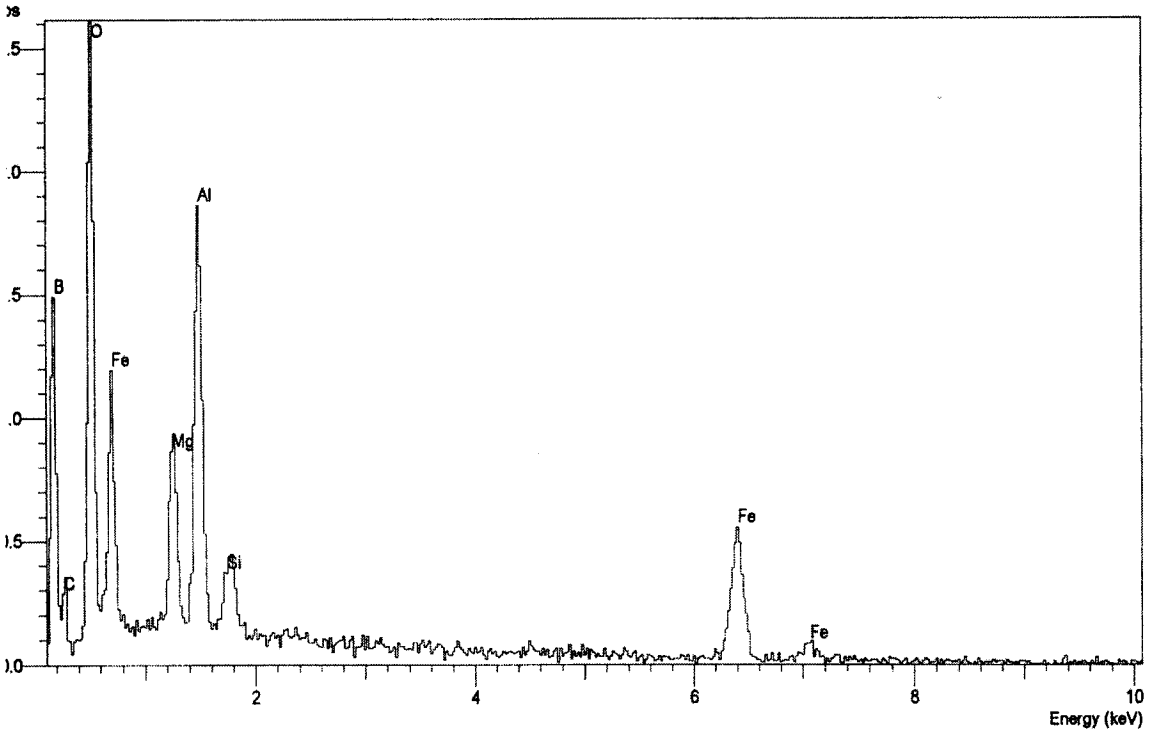

Figure 2.4 (b). EDS spectrum of boride coating

Figure 2.5. Fracture surface showing $AlMgB_{14}$ coating and WC substrate. The left region is WC, and the right uniform thin layer is $AlMgB_{14}$.

Table 2.3 presents Young's modulus and hardness data obtained from the nanoindentation tests. The values are reported for a penetration depth of 80-120 nm, which is believed to avoid the substrate effects. Indentations with contact depths of less than 10-20% of the film thickness are recommended to ensure that the intrinsic properties of the film were not affected by the underlying substrate [13,14]. However, the nanohardness of coating is much lower than that of the microhardness of the bulk boride (32-35 GPa) and this could be due to the non-uniformity of the film and surface roughness caused by particulates.

Figure 2.6 shows the flank wear data of uncoated and coated C-5 carbide inserts in turning AISI 1045 steel bars. The coated tools provided consistent reductions in wear with cutting time although the percentages of wear reduction decreased with an increase in cutting

Table 2.3. Nanoindentation Test Results

Sample	**Calculation Range (nm)**	**Calculation Depth (nm)**	**Hardness (Gpa)**	**Young's Modulus (GPa)**
Uncoated (C-2)	2000	80-120	12.89 ±2.50	381.89± 65.19
Sample M	2000	80-120	20.45 ±2.12	321.17± 57.61

time. On an average, the wear reduction was 12%. This is indeed significant considering the fact that the coating applied is thin (0.5 μm). An increase in coating thickness is expected to further increase the wear performance for two reasons [15]: 1) more volume is available for wear, 2) plastic deformation of the corner radius, responsible for cracking and spallation of the flank face, decreases. The CVD coatings range from 5 to 15 μm in thickness.

Figures 2.7 and 2.8 show the flank and nose wear behavior of coated and uncoated C-2 inserts. The wear curves are nearly linear and do not exhibit "running-in" wear because of the higher cutting speeds used. The improvements in wear reduction are modest in TiB_2, but significant in multilayer, composite $AlMgB_{14}$/ TiB_2 coatings. We believe that the absence of large tool wear reduction with TiB_2 is due to its poor oxidation resistance (it oxidizes at 480°C) [16] or lack of adherence caused by thermal expansion mismatch (thermal expansion coefficient of WC and TiB_2 are 6 (10^{-6}) /K [17] and 8 (10^{-6}) /K [18] respectively). Generally

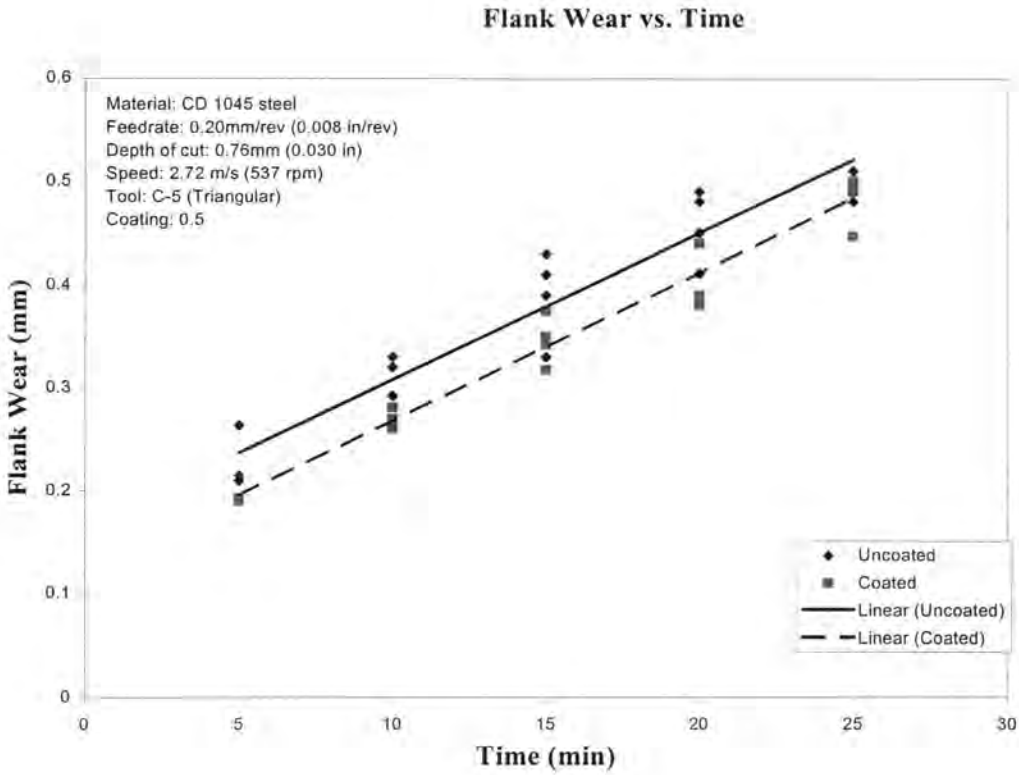

Figure 2.6. Flank wear versus cutting time for uncoated and coated C-5 tool in dry machining.

TiB_2 is applied as diffusion coating to carbide tools in which there is ample time for the formation of CoWB and TiC, which increased the wear resistance by 50% [19]. These diffusion coatings are harder and more wear resistant than CVD - TiC and TiN coatings [20].

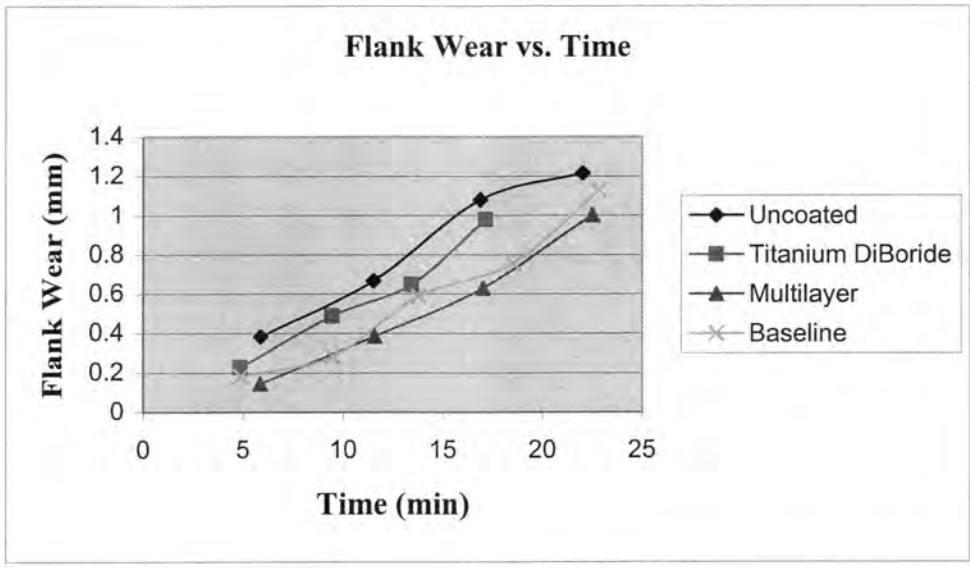

Figure 2.7. Flank wear versus cutting time for uncoated and coated C-2 tools in dry machining.

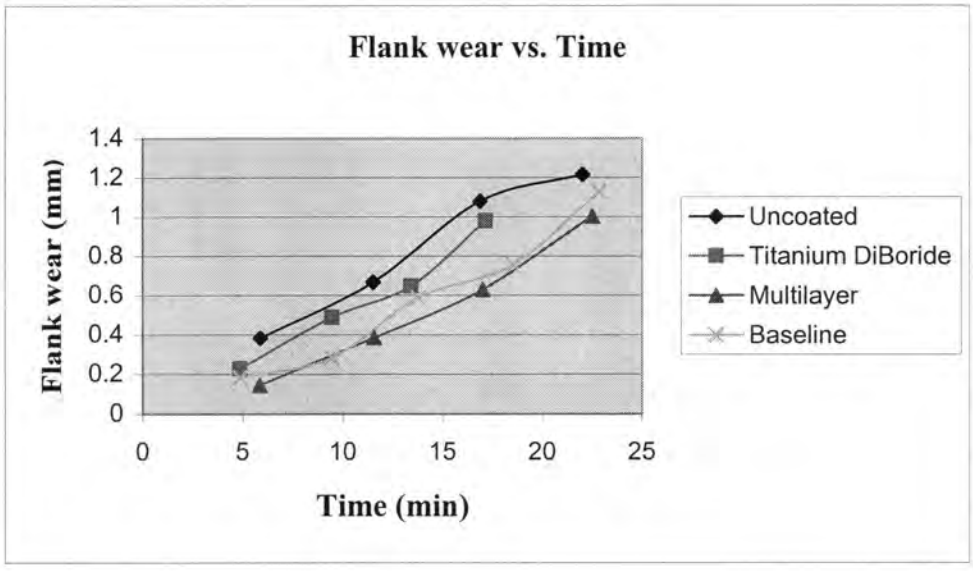

Figure 2.8. Nose wear versus cutting time for uncoated and coated C-2 tools in dry machining.

Figures 2.9 and 2.10 are optical micrographs showing the flank and crater wear patterns respectively. Uncoated tools exhibited significant cratering, which is attributed to the leaching out of cobalt binder from the carbide tool [21]. The flank wear is caused by adhesion and abrasion wear mechanisms, requiring hard, strong material. The improved wear resistance of coated tools in this study is due to higher hardness, adherence of coating to the sharp edges because of the coating's thinness, the presence of aluminum and subsequent formation of chemically and thermally stable Al_2O_3, and development of compressive residual stresses. The marked reduction in wear by multilayer coated tools is attributed to additional abrasion resistance offered by the outer layer TiB_2, interfaces providing energy absorption, and increased thickness. Crater wear is controlled by the diffusion and is governed by the formation of a reaction layer at the interface. The increased performance of multilayer coated tools is due to the formation of TiC or B_4C layer that acts to protect the tool from rapid oxidation and diffusion. Ti-based coatings on carbide tools have been shown to reduce the wear resistance by diffusion and oxidation rather than through by decreasing interfacial friction and chip/tool interface temperature [22,23]. Flank wear of both uncoated and coated tools are said to occur principally by atomic diffusion [22].

Over the past decade, indexable carbide inserts for cutting steels and cast irons are coated with TiC, TiN and Al_2O_3 due to their high resistance to diffusion wear. The coatings have proven to extend the tool life by two to three times [24]. $AlMgB_{14}$ coatings have the potential to outperform Ti-based coatings. For example, the relative merits of physical vapor deposition (PVD) coatings of TiN, TiCN, and TiAlN on a cemented carbide (WC-6%Co, 1700 HV) tool in the turning of 1045 (210 HB) steel were recently reported [2]. TiN and

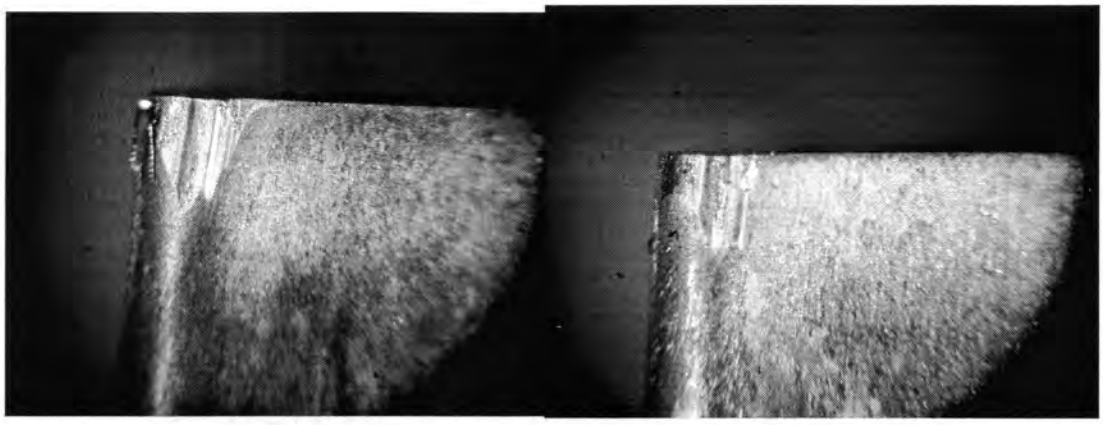

Figure 2.9. Flank wears of (a) uncoated, (b) $AlMgB_{14}$ coated tools

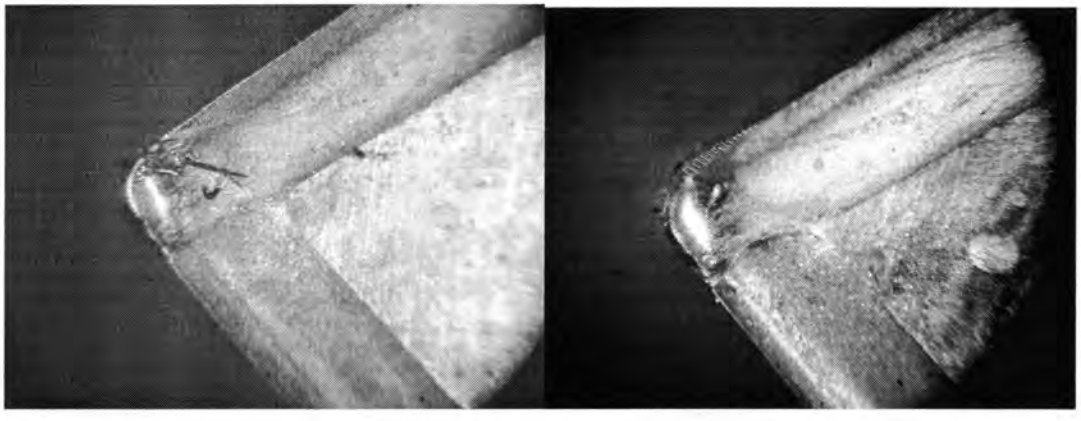

Figure 2.10. Crater wears of (a) uncoated, (b) $AlMgB_{14}$ coated coated tools

TiCN were applied to the inserts by the ion-plating technique while TiAlN was deposited by magnetron-sputtering. The coatings were about 3 μm thick. The turning parameters, except for the cutting speed, were similar to the parameters of the present study and included a feed rate of 0.15 mm and a depth of cut of 0.75 mm. The cutting speed was

made much higher (6 m/sec) because of the application of flood cooling. Flank wear results obtained in this work [2] are comparable to those obtained in the present work.

CONCLUSIONS

Tool coatings increase wear resistance, reduce cutting forces, and lower temperatures at the tool edges, thereby improving productivity and quality. The common coating materials used are TiN, TiCN, and TiAlN. In this paper, it is demonstrated that $AlMgB_{14}$, a new tool coating material applied by the pulsed laser deposition process, has the potential to exceed the performance of Ti-based coatings. PLD, like the traditional PVD processes, is a line-of-sight process capable of coating only the surfaces facing the plasma, and seems to be an ideal process for preserving the stochiometry of $AlMgB_{14}$ during deposition. Thin coatings are strongly adhered to the tool edges at low temperatures (500°C). This work has shown that PLD-deposited $AlMgB_{14}$ has both immediate and future commercial applications in tooling and microelectronics.

ACKNOWLEDGEMENTS

The authors would like to thank NSF for supporting this project under grant DMI0084969. The authors appreciate the assistance of B. A. Cook and J.L. Harringa of Ames Laboratory in providing the $AlMgB_{14}$ target used in this study. The authors also thank Dr. Ashok Kumar, University of South Florida, for conducting nanoindentation tests.

REFERENCES

1. L. Mitoraj, Cutting Tool Engineering, February 2000, V. 52, No.2, 1-5
2. P.C. Jindal, A.T. Santhanam, U. Schleinkofer, A.F. Shuster, and B.K. Marsh, Cutting Tool Engineering, February 1999, Vol.51, No.1, 1-9
3. M. Weiner, Cutting Tool Engineering, February 1999, Vol.51, No.1, 10-18
4. D. Graham, Cutting Tool Engineering, February 1997, V.49, No.1,1
5. W. Pfouts, Manufacturing Engineering, Society of Manufacturing Engineers, July 2000, 98
6. B A. Cook, J. L. Harringa, T. L. Lewis, and A. M. Russell, Scripta Materialia. 42, 597 (2000)
7. C. Belouet, Applied Surface Science, 96-98, 1996, 630-642
8. S. Amirhaghi, Y. Li, J. Kilner, I. Boyd, Journal of Materials Science and Engineering, B34, 1995, 192
9. E.W. Kreutz, M. Alunnovic, T. Klotzblicher, D.A. Wesner, and W.Pfleging, Surface and Coatings Technology, 74-75, 1995, 1012
10. W. Dworschak, K. Jung, and H. Erhardt, Thin Solid Films, 254, 1995, 65
11. E.W. Kreutz, Applied Surface Science, 127-129, 1998, 606
12. A. Sajjadi, K. Kuen-Lau, F. Saba, F. Beech, and I. W. Boyd, Applied Surface Science, 46, 1990, 84
13. T.Y. Tsui, Journal of Materials Research, 14, 6, 1999, 2204
14. J. Wang,, W. Li, H. Li, B. Shi and J. Luo, Thin Solid Films, 366, 2000, 117
15. F. Klocke and T. Krieg, Annals of the CIRP, 48, 2, 1999, 515

16. H.O. Pierson, Journal of Less Common Metals, 67 (1979) 381

17. http://www.insaco.com/MatPages/tungscarb.html

18. K.Otto and A. Schrey, Handbook of Thin Film Process Technology, D. Glocker and

19. S. Shah (eds.), Institute of Physics Publishing, Philadelphia, 1995

20. P. Peshev, Journal of Less Common Metals, 67 (1979) 351

21. G. Bliznakov, Journal of Less Common Metals, 67 (1979) 511

22. A. Chakraborty, K.K. Ray, and S.B. Bhaduri, Materials and Manufacturing Processes, 15, 2, 2000, 269

23. P.A. Dearnley and E.M. Trent, Metals Technology, 9, 1982, 60

24. J.P. Chubb, J. Billingham, D.D. Hall, and J.M. Walls, Metals Technology, July, 1980, 293

25. E.M. Trent and P.K. Wright, Metal Cutting, 4th edition, Butterworth-Heinemann, 2000, 213

CHAPTER 3. TITANIUM MACHINING USING $AlMgB_{14}$-20%TiB_2 COATED CARBIDE INSERTS

A paper submitted for review and publication in the Journal of Machining Science and Technology

Ram Cherukuri and Pal Molian*

Department of Mechanical Engineering, Iowa State University, Ames, IA 50014.

ABSTRACT

Despite several years of research and development, titanium machining remains a challenging task that is currently carried out by the use of straight WC/Co and polycrystalline diamond (PCD) tools. Commercially available coated tools tend to react chemically with titanium, while ceramic tools suffer from chipping and notching. Advancements in cutting tools, particularly coated carbides, are sought to reduce tool wear in machining of titanium alloys. In this work, a recently developed, ultra-hard $AlMgB_{14}$-20%TiB_2 composite material was applied as a coating on WC/6%Co tool inserts by a pulsed laser (excimer) deposition technique. The coating was smooth, continuous, and non-uniform in thickness. The average coating thickness was 0.7 μm for a deposition rate of 0.08 nm per pulse. Nanoindentation tests revealed that the hardness of the coating was approximately twice that of the WC/6%Co substrate. Dry machining tool wear tests, conducted with a CNC lathe by turning bar stocks of heat-treated Ti-6Al-4V alloy, showed that the coated tools outperformed uncoated tools by about two times in flank and nose wears. Detailed analysis of worn tools revealed that the

* Correspondence to molian@iastate.edu

wear mechanisms are quite different in coated tools and are similar to those observed in PCD tools. Results agree well with the general observation that a stable, strong adherent layer forms at the interface between the tool and the chip and minimizes the dissolution-diffusion wear mechanism.

INTRODUCTION

Titanium and its alloys are used extensively in the aerospace industry because of their unique combination of properties, including high strength-to-weight ratio, excellent high-temperature strength, and exceptional corrosion resistance. These alloys are primarily used for applications such as airframes and engine components (fan disks, spacers, shafts and seals). They are also used in petroleum refining, chemical processing, surgical implant manufacturing, pulp and paper industries, nuclear waste storage, food processing, and electronics industries [1]. However, the mechanical and chemical properties of these alloys make them difficult to fabricate by machining and welding. Although near net-shape methods such as precision forging have been developed to minimize machining of titanium components, many parts such as those used in gas turbine engines and airframes are still manufactured by operations such as turning, drilling, and milling to keep the costs low.

Titanium alloys are classified as difficult-to-machine materials for the following reasons [2-12]: 1) the high-temperature strength restricts plastic deformation of metal in the shear zone; 2) the serrated "thin" chips formed during machining create a small contact area resulting in high stresses at the tool edges; 3) the strong chemical affinity of titanium to the

tool materials cause adhesion at cutting temperatures > 500°C; 4) high cutting temperatures develop at the tool tip due to low thermal conductivity, low volumetric specific heat, and "adiabatic or catastrophic thermoplastic shear" mechanism [13-15] and lead to a "flow zone" (also known as "seizure zone") about 10 μm thin between the chip and the tool, and 5) the low modulus of elasticity tends to generate tool chatter and deflection. Consequently, rapid crater and plastic deformation of the cutting edges occur leading to shorter tool life and low permissible metal removal rates [11,12]. The Dissolution-diffusion wear mechanism is found to be mostly responsible for the wear in carbide tools [8] because of the development of high temperatures and considerable chemical activity of titanium. The temperatures generated in titanium machining are much higher than those of steel machining [13]. In addition, even though the tool forces are low, the stress on the rake face is high (because the total chip-tool contact length is very small and the heated region does not extend far along the rake face) and initiates failure at the nose radius of the tool. As a result, the cutting speeds in titanium machining using carbide inserts do not exceed 1 m/sec (200 ft/min) [9].

The past few decades have seen significant advances in cutting tools, including coated carbides, ceramics, cubic boron nitride (CBN), and polycrystalline diamond (PCD). While these have found vast success in machining steels, cast irons, and super alloys, the same degree of success could not be met with titanium alloys [4,5]. For example, the WC/Co tools with coatings of the types TiC, TiCN, TiN/TiC, Al_2O_3/TiC, HfN, and TiB_2 showed greater wear rates than those of straight WC/Co [8,16]. Bhattacharya et al. [17] investigated the performance of fine grain WC/Co grades and triple-coated (TiN/TiC/TiN) carbide tools in machining Ti-6Al-4V and found that tool wear occurred rapidly in coated tools (at high

cutting speeds) due to chemical interactions between the work material and coating layers. Ceramics also found little success in titanium machining due to characteristics such as poor thermal conductivity, low fracture toughness and reactivity with titanium [18]. However, the superhard CBN and PCD have shown good performance in reducing the wear rate [11]. Straight WC/Co grades outperform coated tools in reducing flank, nose and crater wear. The best grade recommended for continuous turning was ISO K20 (ANSI C-2) with a composition of WC-6%Co and medium grain size [19]. It was also found that PCD is an alternative to machine titanium [4,5]. Newer developments include ultra-fine grain WC, CBN, and specific tool geometries, which offer some benefits but are not in common use [4,5].

In this work, we report on a new coating material for carbide inserts, ultra-hard $AlMgB_{14}$-20%TiB_2, and its effects on machining of titanium. This material, which was developed recently, exhibits extreme hardness, high chemical stability, and moderate electrical conductivity [20,21]. Table 3.1 shows the density and hardness of borides [20] along with diamond and CBN. More recently, dry machining tests of bulk $AlMgB_{14}$ showed an unusual absence of tool heating, suggesting that this new family of ultra-hard materials might possess very high thermal conductivity [22]. $AlMgB_{14}$-20%TiB_2 materials are much lighter than other ultra-hard materials. Additionally, the cost of $AlMgB_{14}$ is about 10 to 20 percent of the cost of cubic-BN or diamond. The compound's excellent mechanical properties, combined with its thermal dissipative capability and chemical inertness, may be attributed to its chemistry, crystal structure and intrahedral bonding [21] and make it a superb candidate for a tool material.

In this work, we report the preparation of thin films of $AlMgB_{14}$-20%TiB_2 by a physical vapor deposition (PVD) technique on straight WC/Co tool inserts and the effects of the coating on tool wear in lathe turning of Ti-6Al-4V alloy. Pulsed Laser Deposition (PLD) is used as the PVD technique for synthesis of boride coatings because laser ablation is capable of faithfully reproducing the complex stoichiometry of the borides.

Table 3.1. Density and hardness of selected ultra-hard materials [20]

	Density (g/cm^3)	Hardness (GPa)
C (diamond)	3.52	70
BN (cubic)	3.48	45-50
TiB_2	4.50	30-33
$AlMgB_{14}$	2.66	32-35
$AlMgB_{14}$ + Si	2.67	35-40
$AlMgB_{14}$+ TiB_2	2.70	40-46

PULSED LASER DEPOSITION

PLD is a thin film preparation technique in which an intense laser beam source irradiates a target, creating a directional flux of energetic species that are then deposited onto a substrate positioned at some distance. Compared to other vacuum deposition methods, this is a very elegant and simple technique. PLD has experienced an explosive growth in the last

decade, especially after its success with superconducting oxides. It has been used to prepare high quality dielectric films, epitaxial semiconductor layers, superlattices, and ceramics [23-25].

PLD is applicable to virtually any material. Its most beneficial characteristic is *congruent ablation*, in which, even though the constituents have different vapor pressures, rapid heating of the target and rapid cooling of the film on the substrate prevent the dissociation of source material, leading to stoichiometric films. Another unique feature of PLD is the generation of high-energy, high-velocity particles (ionized and excited species) from the coupling of a large optical field with the solid target, promoting film crystallinity and dense packing. Because some issues are not fully understood, PLD is a scientifically challenging process. Problem areas include laser-target interactions (e.g., evaporation of the target and plasma formation by laser energy absorption, followed by isothermal expansion) and non-equilibrium processes governing the interactions of the species, with the subsequent nucleation and growth of thin film. Additionally, deposition rates are much lower, restricting the rate of production.

Excimer lasers are mostly used for PLD because of their short wavelengths (193-351 nm), high energy per pulse (0.1 to 2 J), and nanosecond (10-30 ns) pulse widths. Of course, Q-switched Nd:YAG lasers in the frequency-tripled or quadrupled modes with pulse duration of 4-12 ns may also be used.

EXPERIMENTAL DETAILS

Work Material

The work material used in the machining experiments was Ti-6Al-4V alloy with a chemical composition (in wt%) Al: 6.21; V: 4.12; Fe: 0.16; C: 0.012; Si: 0.01; Mn: 0.01; Mo: 0.01; and Ti: balance. This alloy accounts for nearly 45% of total titanium production [26]. The alloy was heat treated to a duplex microstructure of α and β phases so that it could be used for high-strength applications at elevated temperatures (between 350 and 400°C). Table 3.2 lists the properties of precipitation-hardened alloy and of AISI 1045 cold drawn steel for comparison purposes. It should be noted that thermal conductivity of titanium is much lower than that of steel.

Table 3.2. Properties of Ti-6Al-4V alloy and AISI 1045 steel [4,5]

Material	Yield Strength, MPa	Young's Modulus, Gpa	Hardness, HV	Density, kg/m^3	Thermal Conductivity, W/m K
Ti-6Al-4V Heat-Treated	965	110	360	4450	7.5
1045 Cold-Drawn steel	530	207	180	7840	51

Tool Material

The throwaway carbide insert of ISO designation CNMG120408 was used for the machining experiments. It is a straight WC-6%Co with a grain size of 1 μm (Grade 883), supplied by Carboloy-Seco, Inc. The tool designation is CNMG 432-MR4, with a negative land geometry and high edge strength. The tool is shaped rhombus with an included angle of 80^{o} and with a chip-breaker groove. The tool geometry consists of rake angle -6^{o}, relief angle 6^{o}, lead angle 13^{o}, and nose radius of 0.8 mm (1/32 in.)

Coating Material

The $AlMgB_{14}$-20%TiB_2 targets were made in the Ames Laboratory (affiliated with Iowa State University) by mixing 2.24 gm of B, 0.36 gm of Mg, 0.75 gm of TiB_2 and 0.4 gm of Al and ball milling the mixture for 16 hours. The part was then subjected to uniaxial hot pressing and sintering at $1400^{o}C$ for 60 minutes. The target was then polished and made available in the form of 12-mm diameter, 3-mm thick discs. The hardness was measured as 4000 HV (nominal value) using the Tukon microhardness tester.

Laser

Excimer laser was used to perform the deposition experiments. The specifications of the laser are presented in Table 3.3.

Table 3.3. Excimer laser specifications

Type	Wavelength	Pulse Energy	Pulse Width	Repetition Rate	Beam Size
KrF	248 nm	300 mJ (max)	23 ns	100 Hz (max)	23 mm x 12 mm

Tool Coating using Pulsed Laser Deposition

The surfaces of tool inserts were degreased using acetone/methanol sequence in an ultrasonic cleaner and then dried using nitrogen. The tool was mounted inside a high vacuum (10^{-6} torr) stainless steel chamber that has provisions for laser beam transmission, gas flow, and heating of the substrate, as well as a quartz window for viewing the plasma during the coating process. The target, $AlMgB_{14}$ doped with 20-wt% TiB_2, was secured on a support provided for this purpose in the chamber. The tool insert, placed opposite to the target, was pre-heated to 500°C using a resistance heater. The laser beam was focused through a 150-mm focal length lens and directed at 45° to the target. The target was rotated using a magnetic controlled device so that during ablation, the laser beam strikes the target evenly without cratering at one spot. The deposition process was facilitated by a computerized control system in which the laser parameters (power, pulses), target rotation, target-to-substrate distance, and substrate temperature were all controlled. The following parameters were used in the coating process: pulse energy = 200-250 mJ; pulse repetition rate = 5 Hz; spot size = 2 mm^2; substrate-to-target distance ~33, mm and deposition time = 30 min.

Scanning Electron Microscopy Analysis

The coated tools were analyzed in a scanning electron microscope (JEOL 840A) coupled with an electron probe microanalyzer (EPMA), operated in the secondary electron mode at 10 kV. The tool was also fractured and then examined for film thickness and interface bonding between the substrate and the coating. The composition of the film was estimated by using EPMA to analyze the elements present in the coating.

Nanoindentation

Nanoindentation tests have been used recently to evaluate the mechanical properties of materials over smaller scales. This depth-sensing indentation method is used at low loads and is a well-established technique for investigating of localized mechanical behavior of materials. Nanoindentation testing with a Berkovich diamond indenter (a three-sided pyramid with an area-to-depth function the same as that of a Vicker's indenter) was used to measure the hardness and elastic modulus of thin films. In this test, the load was gradually increased to a pre-set maximum value such that both elastic and plastic deformation occurred in the thin film. The load was then released, causing partial or complete relaxation. The unloading was dominated by elastic displacements. Nanohardness and modulus were obtained from the load-displacement curves. First, the contact depth h_c and the contact stiffness S were determined from load-displacement curves. Second, the hardness H and the modulus E were calculated. Contact depth h_c is given by:

$$h_c = h_t - \frac{\varepsilon F}{S}$$

where h_t is maximum depth of penetration including elastic deformation of the surface under load, F is the maximum force, and $\varepsilon = 0.75$ is a geometrical constant associated with the shape of the Berkovich indenter. Once h_c is determined, the projected area A of actual contact can be calculated from the cross-sectional shape of the indenter along its length. S is obtained by use of the following equation:

$$S = \frac{dF}{dh} = \frac{2}{\sqrt{\pi}} E_r \sqrt{A} \ ,$$

where E_r is the reduced modulus. Hardness is then calculated from the simple relation:

$$H = F/A$$

The reduced modulus E_r is defined as:

$$\frac{1}{E_r} = \frac{1-\nu^2}{E} + \frac{1-\nu_i}{E_i}$$

where E and ν are Young's modulus and Poisson's ratio for the sample and E_i (1141 GPa) and ν_i (0.07) are the same for the indenter respectively.

Machining Tests

Single-point turning tests were conducted using a Hitachi Seiki HT 20SII CNC turning center. The lathe has the provision to keep the surface speed constant while the diameters are being reduced. The workpiece was a solid cylinder of approximately 76 mm diameter and 300 mm length. Bars were discarded when the diameter was reduced to 25 mm. No coolant was used during the experiments. The speed and feed were kept constant throughout the experiments. The machining parameters are listed in Table 3.4. After each pass the tool was removed from the tool post. Because of the decrease in diameter, the

average time taken for each pass varied. The flank and nose wears were measured using Gaertner Scientific toolmaker's microscope with a magnification of 30X. Tests were repeated three times. The ISO's criteria [27] used for tool life that included average flank wear 0.4 mm, nose wear 1.0 mm, crater wear depth 0.14 mm, and surface roughness 6 μm Ra. The surface roughness was determined using a surface profilometer. The tool wear was characterized by SEM.

Table 3.4. Machining Parameters

Feed	0.1524 mm/rev (0.006 in/rev)
Cutting speed	61 m/min (200 ft/min)
Depth of cut	0.76 mm (0.03 in.)
Cutting length	280 mm (11 in.)

RESULTS AND DISCUSSION

Figure 3.1 is an SEM micrograph of the cross-section of laser-deposited $AlMgB_{14}$-20%TiB_2 film, showing that the film thickness, on the average, is 0.7 μm. The film is non-uniform in thickness but is continuous and free of porosity and inclusions. For an energy fluence of 10 J/cm^2, the deposition rate was 0.08 nm per pulse, consistent with those reported in the literature [23-25].

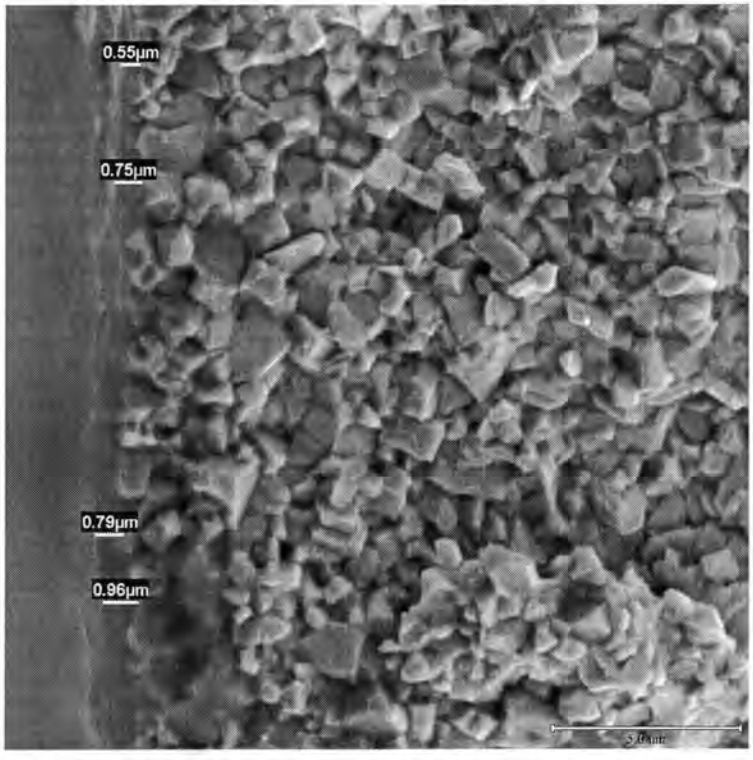

Figure 3.1. SEM micrograph of transverse section (obtained by fracturing the tool) of laser- deposited thin film of $AlMgB_{14}$-20%TiB_2

Figures 3.2 and 3.3 are the nanoindentation curves of Young's modulus and hardness *versus* penetration depth obtained by employing the continuous measurement techniques. The high values near the surface are due to "skin" effect or artifact. With increasing penetration, values go through a minimum and then began to increase again because of the influence of the underlying substrate. For a penetration depth of 80-120 nm (which avoids the substrate effects), the hardness and Young's modulus of coated tool are 22 ±7 GPa and 480 ±194 Gpa, respectively. By comparison, the respective values of the uncoated substrate

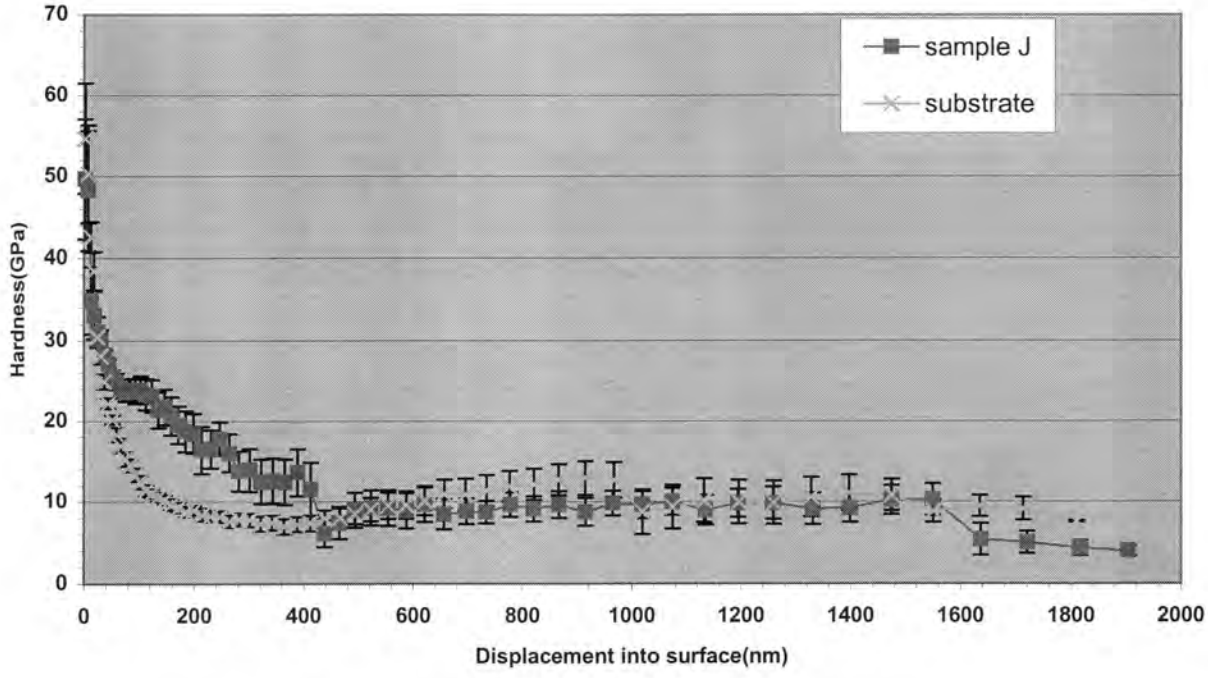

Figure 3.2. Nanoindentation hardness vs. penetration depth

are 13 ±3 GPa and 382 ±65 GPa. The nanohardness of coating is much lower than that of the microhardness of the bulk boride. This could be due to the substrate effects. Indentations with contact depths of less than 10-20% of the film thickness are recommended to ensure that the intrinsic properties of the film were not affected by the underlying substrate [28,29]. Of course, models and theories have been developed in an attempt to explain and predict such depth dependence of the indentation hardness and elastic modulus; however, they are limited to only specific material systems [29]. If the film is harder than the substrate, as in this case, then most of the plastic deformation is on the soft substrate. Therefore, these hardness results do not truly reflect the mechanical properties of the film because of the significant contribution from the substrate deformation and surface roughness caused by particulates on

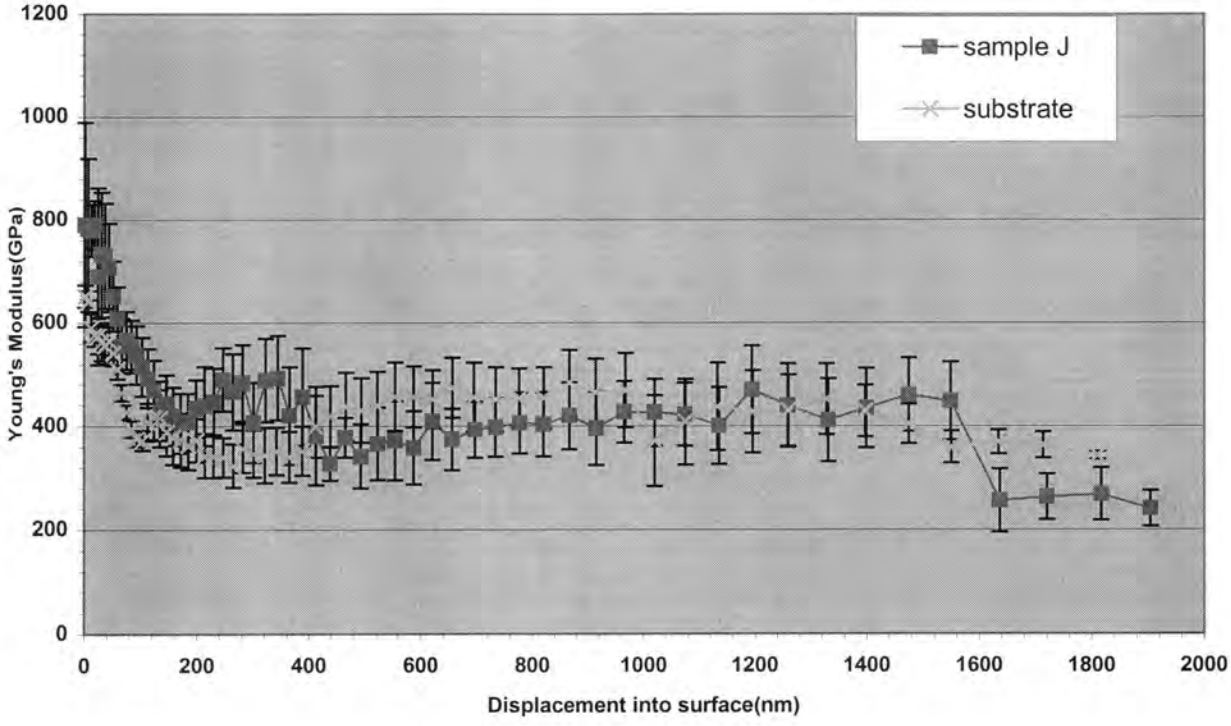

Figure 3.3. Young's modulus vs. penetration depth

the film. In addition, the large variations of the data are attributed to non-uniform thickness and surface roughness caused by particulates.

Figures 3.4 and 3.5 show the progression of average nose and flank wears with time for uncoated and coated tools. The wear curves can be divided into two regions, constant wear and accelerated wear, which are chiefly determined by interplay among cutting forces, compressive stresses, and temperatures. The constant wear region is caused by reduction in cutting forces and stresses usually observed in the initial stages of cutting and attributed to the geometric conformity of the contacting surfaces [9]. The accelerated wear is essentially due to the substantial temperature rise in the cutting zone. Similar wear curves are reported

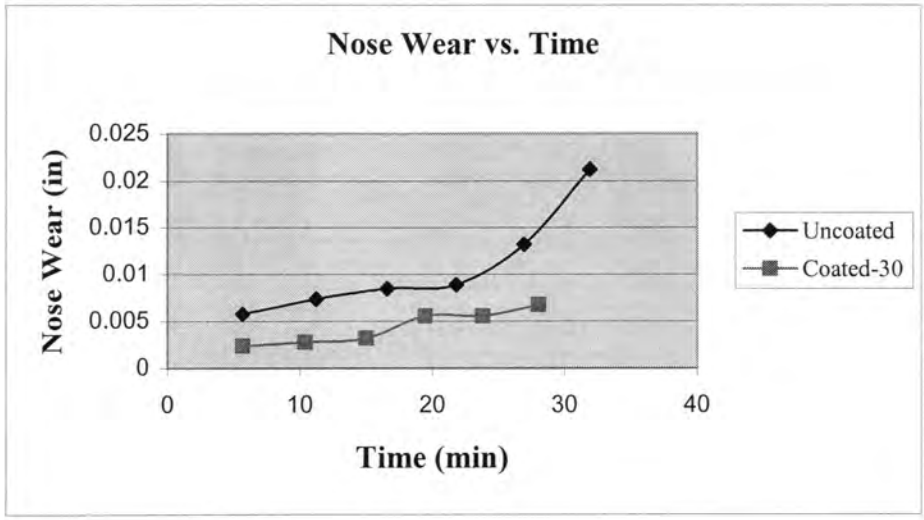

Figure 3.4. Nose wear vs. time

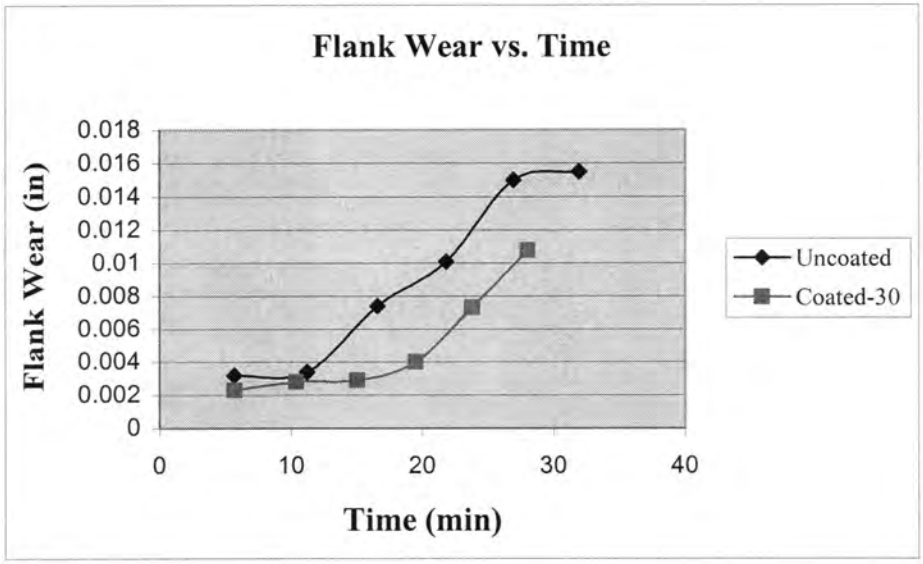

Figure 3.5. Flank wear vs. Time

for titanium machining at cutting speeds < 60 m/min [10]. However, at higher cutting speeds (>80 m/min), the constant wear region disappeared [5]. Another observation is that the wear at the flank face and the nose were nearly equal in the initial stages. However, the wear increased faster at the nose than at the flank face in the later stages. This could be a result of high temperatures leading to deformation and other types of wear mechanisms. Nose wear seems to be the governing factor in limiting tool life. The key result of Figures 3.4 and 3.5 is that the ultra-hard boride coating enabled a reduction of 60% (average) nose wear and 40% (average) flank wear, implying a marked improvement in tool life.

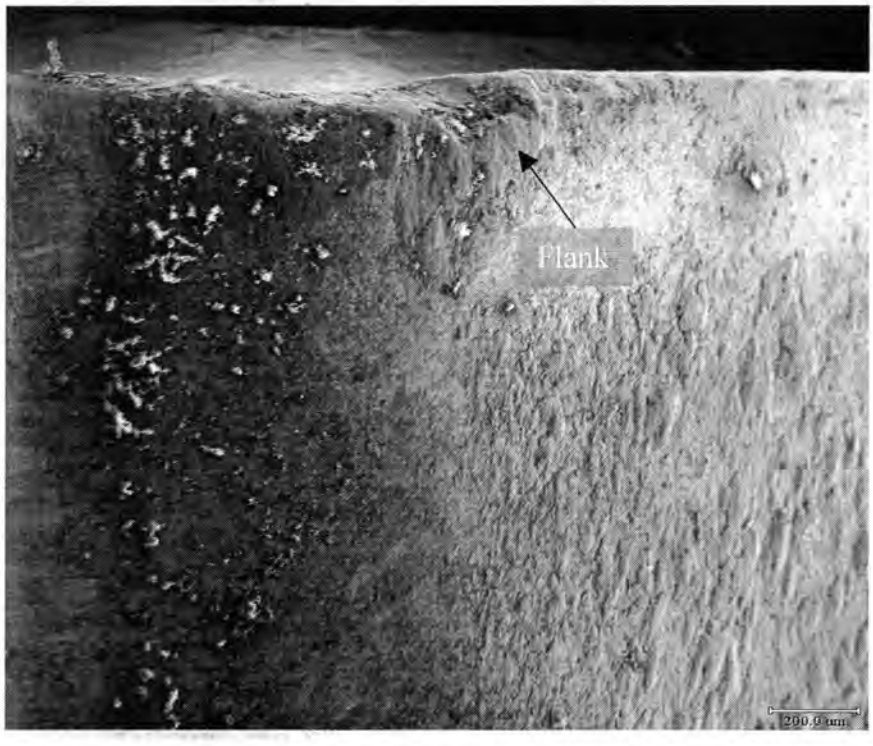

Figure 3.6. Flank wear on uncoated tool (50x)

SEM analysis of worn-tools revealed that different wear mechanisms are associated with coated and uncoated tools. In the case of uncoated tools (Figure 3.6), large amount of wear debris and deformation of the nose are readily seen. Attrition of fine WC grains, abrasion (caused by the chipped material between the tool's flank face and the newly machined surface), extensive plastic deformation, and dissolution of the material appear to be the controlling wear mechanisms. These types of wear are attributed to the high-temperatures resulting from significant heat transmission through the tool and to the high stresses developed at the tool edge by the formation of thin segmented chips with short chip-tool contact length. Tlusty [30] has analyzed the temperature fields at the contact between the chip and the tool using finite-difference computations with simplifying assumptions for alloys including Ti-6Al-4V. The assumptions involved in this analysis are: 1) there is no heat transport from shear plane into the workpiece; 2) the change in thermal properties with temperature is ignored. These errors are said to be within 20% at most, and much less in many cases [30]. This model has been applied to the present case, and results show a maximum temperature of 1348 K along the tool-chip contact length. The data are also consistent with experimentally measured cutting temperatures in titanium machining [9,13].

Because titanium alloys are much more resistant to heat than steel, the tool experiences thermal softening and consequent deformation of the cutting nose. The phase transition of titanium from HCP to BCC at 1153 K aggravates the situation by increasing the shear strain and subsequently raising the tool edge temperature. Another aspect is the oscillations produced by the low and high shear strain regions of the chip formation leading to an increase in frictional heating. It has been shown that the edge deteriorates rapidly when

the tool temperature reaches about 1000 K [9]. Thus, the uncoated tool wear mechanisms in titanium machining are essentially thermal in nature, with characteristics such as thermal deformation of the edge and dissolution of WC in titanium.

In the case of coated tool, the wear is low, uniform and smooth (Figure 3.7), with little evidence of plastic deformation and abrasion. The "uniform flank wear" is the most desirable because it could be very well predicted. The high hardness of the coating withstood the high stresses developed in the cutting zone and resisted the deleterious effects of segmented chip formation of titanium. The dissolution is also reduced by the formation of a reactive layer, which is confirmed by the EPMA analysis (Figure 3.8). Although the exact composition of this reactive layer is unknown at present, it is believed that formation of this

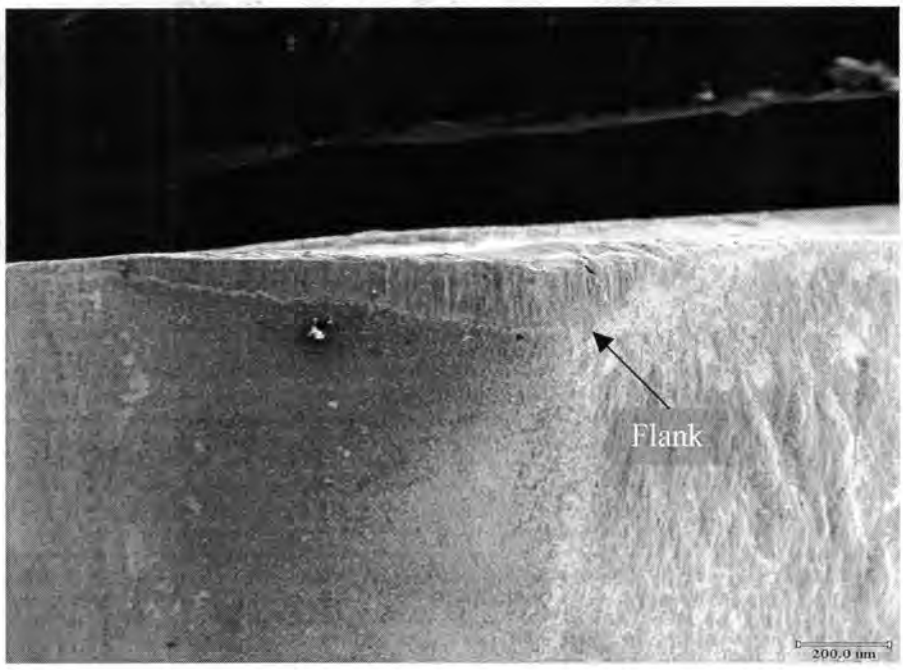

Figure 3.7. Flank wear on coated tool (50x)

layer provided a thermal barrier that minimizes thermal gradients and thermal shock, and also prevented attrition.

Figures 3.9 and 3.10 show that the crater wear of coated tool is slightly less than that of uncoated tool. The crater wear in both cases is relatively small because of the low cutting speed. The diffusion and dissolution processes that occur across the tool-chip interfaces determine the extent of crater wear [4,5,8]. In the case of uncoated WC/Co tools (as in PCD

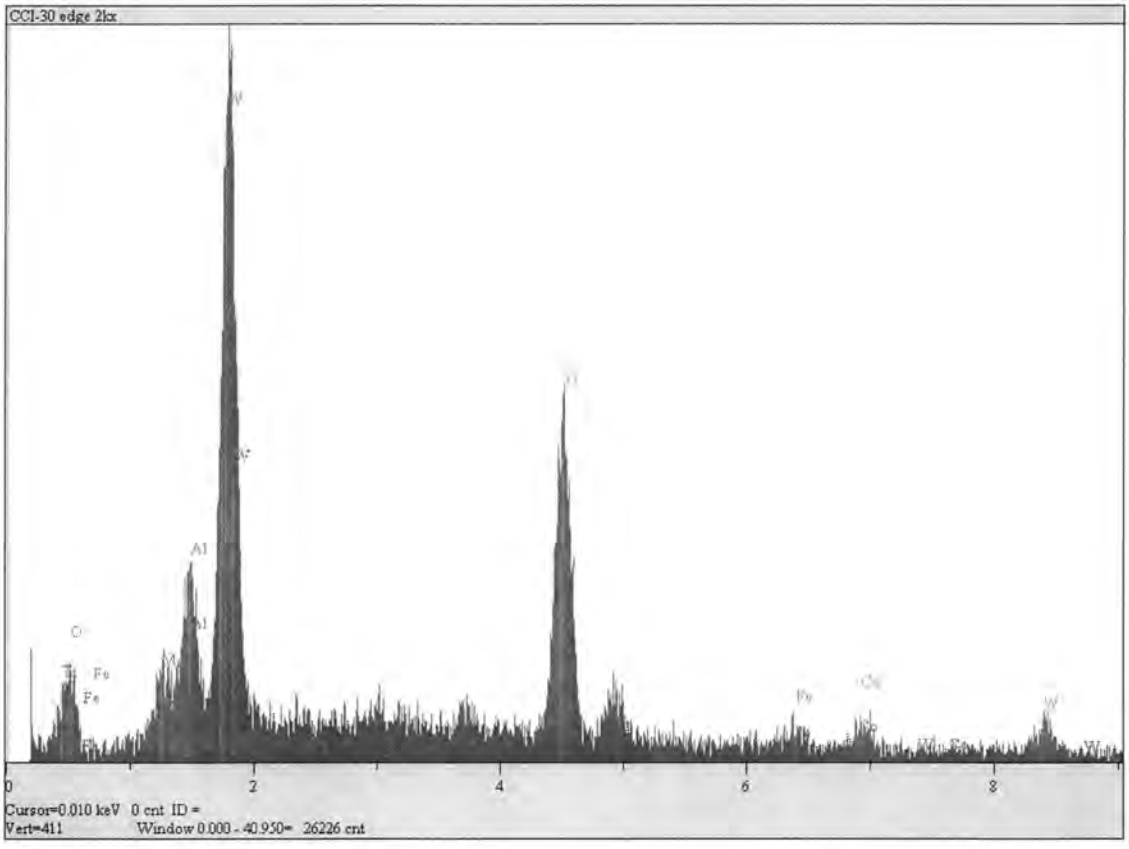

Figure 3.8. X-ray spectrum of elements present at the tool wear interface.

tools), a stable reaction layer of TiC is formed at the interface between the tool and the chip. This TiC layer, with a typical thickness of 100 nm, has a high deformation resistance and strong adherence to both the chip and the tool [4,5,8]. However, one must note that the beneficial effect of the TiC layer formed contradicts the findings that CVD-TiC coatings were not effective in combating tool wear in titanium machining. The thickness of the reaction layer is decided by the competition between the diffusion flux of tool species through this layer and chemical dissolution of the reaction layer with the chip (dissolution-diffusion wear). Once this layer reaches a critical thickness, it can minimize the mass transportation of species from the tool into the chip, thus reducing the wear rates. The strong adhesion of this layer also prevents the physical motion of the tool/chip interface, reducing

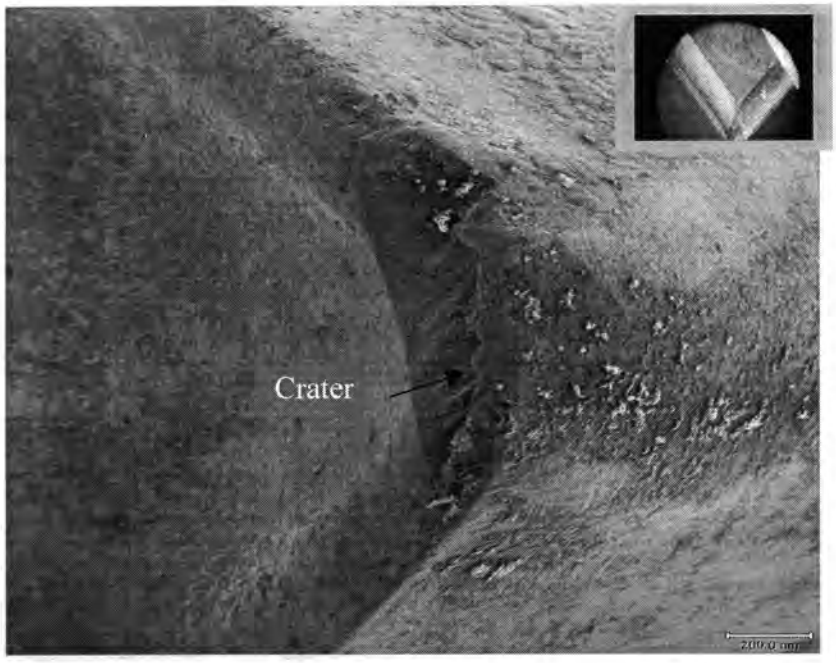

Figure 3.9. Crater wear on uncoated tool (50x)

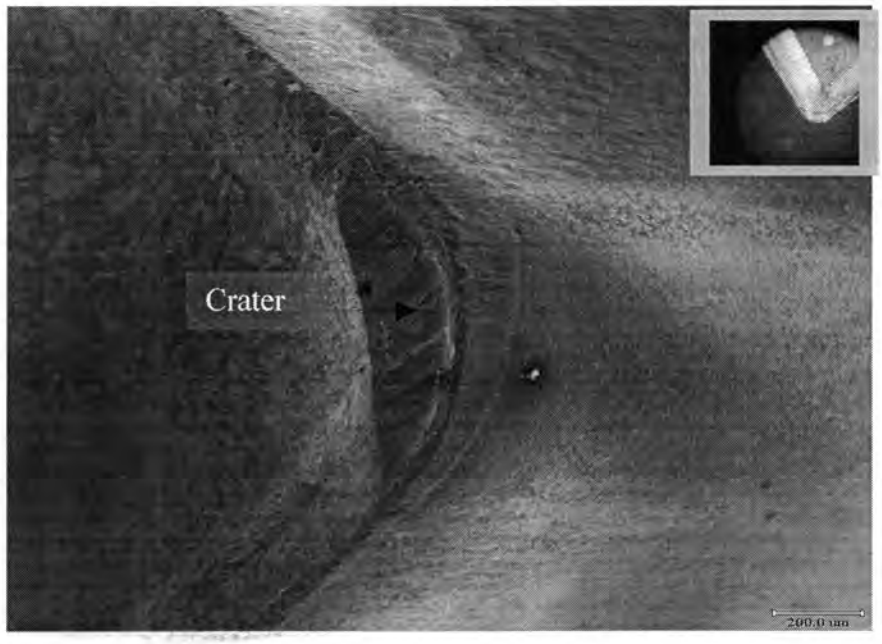

Figure 3.10. Crater wear for coated tool (50x)

attrition [8]. It has been reported that CBN cutting of titanium generated a stable, adherent layer similar to TiC and prevented the diffusion of tool into the chip [13]. This reaction layer formed, grew with cutting time, and remained attached to the tool until the stress caused the failure [13]. Similar grounds could also explain the results of the present study in that formation of a layer (possibly AlB/TiB_2) at the interface that reduced crater as well as flank and nose wears.

Figure 3.11 shows the surface roughness data of uncoated and coated tools. Surface roughness of boride coating is comparable to or better than that reported by CBN tools for the same cutting speed [9].

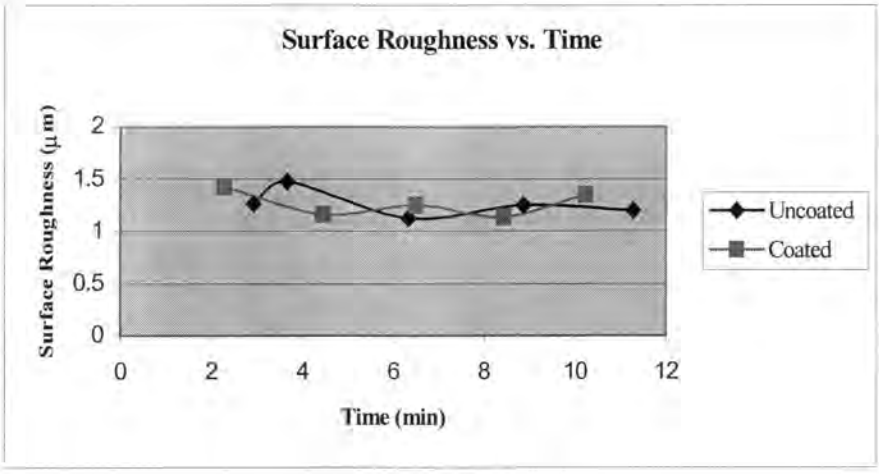

Figure 3.11. Surface Roughness of Titanium

CONCLUSIONS

Ultra-hard boride coated tools proved to be effective in minimizing tool wear in titanium machining. Boride coated tools limited the dissolution-diffusion wear mechanism caused by thermal effects. These tools have advantages over traditional coated tools of the type TiN, TiC, Al_2O_3, and HfN and are comparable to PCD and CBN tools without localized chipping, notching, or cracking. This study is the beginning of a whole new generation of ultra-hard, boride-coated tools that not only are cost effective but also offer superior performance.

ACKNOWLEDGEMENTS

The authors would like to acknowledge the National Science Foundation (NSF) for supporting this research work under grant DMI-0084969. Thanks are also due Dr. Ashok Kumar, University of South Florida, for nanoindentation tests.

REFERENCES

1. J.R. Myers; H.M. Bomberger; and F.H. Froes. Corrosion Behavior and Use of Titanium and its Alloys. *Journal of Metals*, 36 (10), 1984, 50
2. N. Zlatin. *Modern Machine Shop*, 1970, 42(12), 139
3. N.H. Cook. Proceedings of Symposium on *Machining and Grinding of Titanium,* Watertown Arsenal, Watertown 72, Massachusetts, 31 Mar.1953, 1
4. E.O. Ezugwu; Z.M. Wang. Titanium alloys and their machinability – a review. *Journal of Materials Processing Technology*, 68, 1997, 262-274.
5. A.R. Machado; J. Wallbank. Machining of titanium and its alloys – a review. Proceedings of Institution of Mechanical Engineers, 204, 1990, 53-60.
6. R. Komanduri. Some clarification on the mechanics of chip formation when machining titanium alloys. *Wear*, 76, 1982, 15
7. R. Komanduri; B.F. Von Turkovich. New observations on the mechanism of chip formation when machining titanium alloys. *Wear*, 69 (48), 1982, 179-188.

8. P.D. Hartung; B.M. Kramer. Tool wear in titanium machining. *Annals of CIRP*, 31(1), 1982, 75-80.

9. Z.A. Zoya; R. Krishnamurthy. The performance of CBN tools in the machining of titanium alloys. *Journal of Materials Processing Technology*, 100, 2000, 80-86.

10. A. Jawaid; C.H. Che-Haron; A. Abdullah. Tool wear characteristics in turning of titanium alloy Ti-6246. *Journal of Materials Processing Technology*, 92-93, 1999, 329-334.

11. P.A. Dearnley; A.N. Grearson. Evaluation of principal wear mechanisms of cemented carbides and ceramics used for machining titanium alloy IMI 318. *Materials Science and Technology,* 2, 1986, 47

12. N. Narutaki; A. Murakoshi. Study on machining of titanium alloys. *Annals of CIRP*, 32 (10) 1983, 65-69.

13. S. K. Bhaumik; C. Divakar; A.K. Singh. Machining Ti-6Al-4V alloy with a wBN-cBN composite tool. *Materials and Design*, 16 (4), 1995, 221-226.

14. R.F. Recht. Trans. ASME, *Journal of Applied Mechanics*, June 1964, 189

15. B.F. Von Turkovich. Shear stress in metal cutting. *Journal of Engineering for Industry*, Feb.1970, 151

16. D. Eylon; S. Fulishiro; P.J. Postans; F.H. Froes. High-Temperature Titanium Alloys – A Review. *Journal of Metals*, 36, 1984, 55

17. S.K. Bhattacharyya; I.R. Pashya; R. Ezugwu; A.R. Machado. Eighth CBECIMT (Engineering and Materials Science Brazilian Conference), UNICAMP, Campinas, SP, Brazil, 12-15 Dec.1988, 271

18. J. Kertesz; R.J. Pryor; D.W. Richerson; R.A. Cutler. Machining Titanium Alloys with Ceramic Tools. *Journal of Metals*, 40 (5), 1988, 50

19. P.A. Dearnley; A. N. Grearson; J. Aucote. Wear Mechanisms of cemented carbides and ceramics used for machining titanium. *High Tech Ceramics*, 38, 1987, 2699

20. B.A. Cook; J. L. Harringa; T. L. Lewis; A. M. Russell. A new class of ultra-hard materials based on $AlMgB_{14}$. *Scripta Materialia*, 42, 6, 2000, 597

21. B.A. Cook; J. L. Harringa; T. L. Lewis; A. M. Russell. Private communication.

22. B.A. Cook; J. L. Harringa; A. M. Russell; I. E. Anderson; S. A. Batzer. *Wear, in press.*

23. C. Belouet, Thin film growth by the pulsed laser assisted deposition technique. *Applied Surface Science*, 96-98, 1996, 630

24. D. B. Chrisey; G.K. Hubler (eds.). Pulsed Laser Deposition of Thin Films. Wiley-Interscience, New York, 1994

25. E.W. Kreutz. Pulsed laser deposition of ceramics – fundamentals and applications. *Applied Surface Science*, 127-129, 1998, 606

26. R.A. Wood; R.J. Favor. Titanium Alloys Handbook. AirForce Materials Laboratory, Wright-Patterson Air Force Base, OH 45433, 1972

27. ISO, Tool life testing with single-point turning tools, ISO 3685, 1977

28. T.Y. Tsui, J. Vlassak, W.D. Nix. Indentation plastic displacement field: Part II. The case of hard films on soft substrates. *Journal of Materials Research*, 14 (6), 1999, 2204

29. J. Wang; W. Li; H. Li; B. Shi; J. Luo. Nanoindentation study on the mechanical properties of Tic/Mo multilayers. *Thin Solid Films*, 366, 2000, 117

30. G. Tlusty. Manufacturing Processes and Equipment, Prentice Hall, 2000, 442.

CHAPTER 4. GENERAL CONCLUSION

The feasibility of nano-crystalline thin film depositions of $AlMgB_{14}$ carbide tools using pulsed laser deposition technique has been verified. The characteristics of the films were studied using SEM techniques and analyzed. The wear rate of the coated carbide tools decreased by about 15% when compared with uncoated C-5 tools and wear rate of coated carbide C-2 tools reduce by about 25% when compared to uncoated C-2 tools during the machining of 1045 steels and hence it indicates that $AlMgB_{14}$ has great potential for coating carbide tool inserts. In the case of machining of titanium, the average nose wear of coated tools was about 60% less compared to uncoated tools and the average flank wear was 40% compared with uncoated tools. The results obtained prove that the super hard material has a great potential usage in developing tools with more wear resistance.